

# Flexible mechanical metamaterials

Katia Bertoldi<sup>1</sup>, Vincenzo Vitelli<sup>2,3</sup>, Johan Christensen<sup>4</sup> and Martin van Hecke<sup>5,6</sup>

**Abstract** | Mechanical metamaterials exhibit properties and functionalities that cannot be realized in conventional materials. Originally, the field focused on achieving unusual (zero or negative) values for familiar mechanical parameters, such as density, Poisson's ratio or compressibility, but more recently, new classes of metamaterials — including shape-morphing, topological and nonlinear metamaterials — have emerged. These materials exhibit exotic functionalities, such as pattern and shape transformations in response to mechanical forces, unidirectional guiding of motion and waves, and reprogrammable stiffness or dissipation. In this Review, we identify the design principles leading to these properties and discuss, in particular, linear and mechanism-based metamaterials (such as origami-based and kirigami-based metamaterials), metamaterials harnessing instabilities and frustration, and topological metamaterials. We conclude by outlining future challenges for the design, creation and conceptualization of advanced mechanical metamaterials.

Metamaterials are carefully structured materials — often consisting of periodically arranged building blocks — that exhibit properties and functionalities that differ from and surpass those of their constituent materials rather than simply combining them. In the past two decades, metamaterials that manipulate optical<sup>1</sup>, acoustic<sup>2</sup> and thermal<sup>3</sup> fields and that have highly unusual properties, such as a negative refraction index, have been demonstrated. This has led to new applications, such as perfect lenses<sup>4</sup>.

Mechanical metamaterials constitute a more recent branch of metamaterials research that exploits motion, deformations, stresses and mechanical energy<sup>5,6</sup> (FIG. 1). Although they borrow design ideas from wave-based metamaterials, they also provide new challenges and opportunities. For example, both wave-based and mechanical metamaterials can use geometry to obtain zero or negative material parameters<sup>7–18</sup>, but in the context of mechanical metamaterials, several recent designs have also harnessed shape morphing<sup>19–35</sup>, topological protection<sup>36–61</sup>, instabilities and nonlinear responses<sup>62–74</sup> to obtain advanced functionalities. Auxetic materials — that is, materials that either expand or contract in all directions when a force is applied — are an early example of mechanical metamaterials and illustrate well how structure controls the behaviour of mechanical metamaterials (BOX 1).

The building blocks of mechanical metamaterials — the meta-atoms — deform, rotate, buckle, fold and snap in response to mechanical forces and are designed such that adjacent building blocks can act together to yield a desired collective behaviour. A cornerstone for the design of both meta-atoms and metamaterials are slender elements (FIG. 1). As the bending stiffness of these

elements scales with the third power of their thickness, very strong stiffness heterogeneities can be designed and realized by using various additive manufacturing techniques. These heterogeneities underlie the qualitative differences between the global properties of metamaterials and those of their constituent materials. Thus, carefully designed architectures can be used to achieve any combination of linear elastic coefficients that is not forbidden by thermodynamics. Often such heterogeneities are used to approximate hinging elements, leading to nearly freely hinging structures featuring floppy modes and mechanisms<sup>75</sup>. As we discuss in this Review, a wide variety of metamaterial designs exploit this principle, in particular, origami, kirigami and shape-shifting materials. Slender elements allow for large deformations, leading to geometric nonlinearities, and are prone to elastic instabilities, such as buckling and snapping (FIG. 1). Nonlinearities and instabilities underlie several advanced metamaterial functionalities, such as multistability and programmability. Finally, topological phases have recently been created in suitably designed mechanical structures. The properties of these metamaterials are topologically protected — that is, they are robust against smooth deformations of the material. We conclude this Review by outlining the key challenges for future work.

## Linear mechanical metamaterials

**Linear elastic metamaterials.** Isotropic materials are described by two elastic coefficients, such as the Poisson's ratio and Young's modulus, whereas for anisotropic materials, the elasticity tensor can contain up to 21 independent coefficients, providing a large target space

<sup>1</sup>Harvard John A. Paulson School of Engineering and Applied Sciences, Harvard University, Cambridge, Massachusetts 02138, USA.

<sup>2</sup>Instituut-Lorentz, Universiteit Leiden, Postbus 9506, 2300 RA Leiden, The Netherlands.

<sup>3</sup>James Franck Institute and Department of Physics, The University of Chicago, Chicago, Illinois 60637, USA.

<sup>4</sup>Instituto Gregorio Millán Barbany, Universidad Carlos III de Madrid, Avenida de la Universidad 30, 28916 Leganés (Madrid), Spain.

<sup>5</sup>AMOLF, Science Park 104, 1098 XG Amsterdam, The Netherlands.

<sup>6</sup>Huygens-Kamerlingh Onnes Laboratories, Universiteit Leiden, Postbus 9504, 2300 RA Leiden, The Netherlands.

Correspondence to J.C. [johan.christensen@uc3m.es](mailto:johan.christensen@uc3m.es)

doi:10.1038/natrevmats.2017.66  
Published online 17 Oct 2017

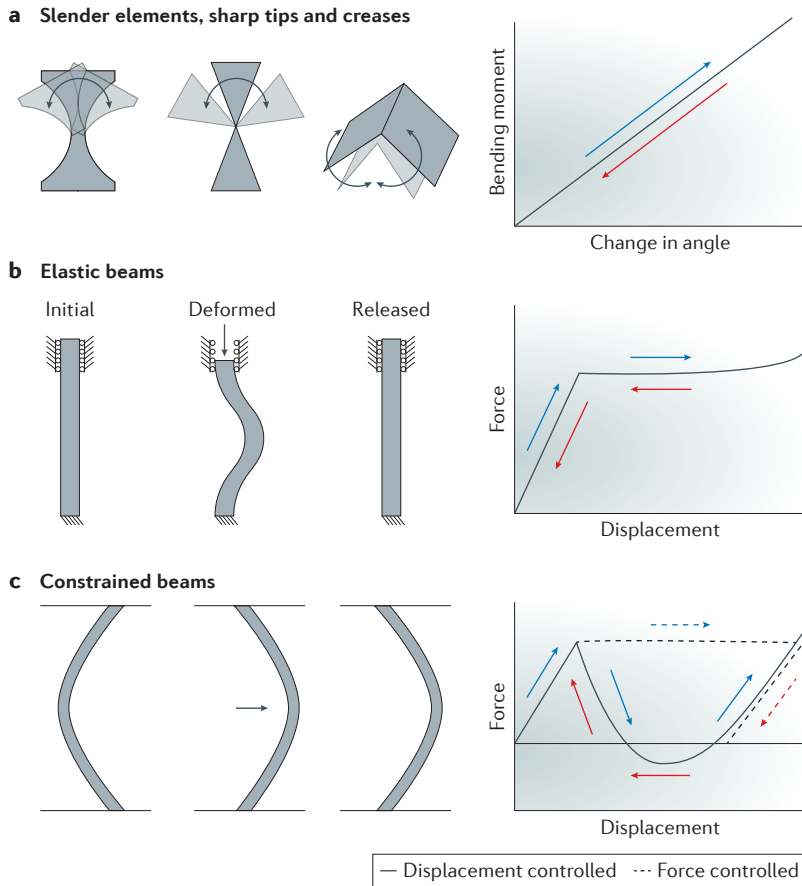


**Figure 1 | Building blocks of mechanical metamaterials.** **a** | Slender elements, sharp tips and creases localize bending; the bending moment increases monotonically with the angle. **b** | Elastic beams undergo a buckling instability when axially compressed and fully recover their initial shape when unloaded; this instability provides nonlinear but reversible building blocks for metamaterials. **c** | Constrained beams can jump to a different equilibrium state through rapid snap-through buckling. Snapping is often accompanied by bistability, depending on the geometry, amount of confinement and boundary conditions; for example, experiments in which the external deformations are controlled may result in a different response than in experiments in which the external forces are controlled (solid and dashed arrows, respectively). Hence, under force-controlled conditions, such elements provide bistable building blocks with hysteretic behaviour.

for mechanical metamaterials design. This is because the basic quantities in mechanics, stress ( $\sigma_{ij}$ ) and strain ( $e_{kl}$ ), are symmetric  $3 \times 3$  tensors, related through the rank-four elastic tensor  $C_{ijkl}$ :

$$\sigma_{ij} = C_{ijkl} e_{kl} \quad (1)$$

In 1995, Milton and Cherkav showed that it is possible to design architectures consisting of ordinary elastic materials and vacuum to create metamaterials with any form of  $C_{ijkl}$  that is not forbidden by thermodynamics<sup>10</sup>. Auxetic materials are one example of metamaterials with unusual  $C_{ijkl}$ . Extremal materials, which resist only one type of deformation (BOX 1), and pentamode materials — a particular type of extremal material — constitute another example. Pentamode materials are defined as having five of the six eigenvalues of the elasticity tensor in the Mandel notation equal to zero, which implies that most  $C_{ijkl}$  coefficients are zero<sup>10</sup>. A striking example of a

pentamode material is a structure in which the ratio of the bulk-to-shear elastic modulus diverges; like a fluid, such a material does not resist shear and only resists volumetric deformations<sup>10</sup>. Advances in additive manufacturing have enabled the creation of 3D extremal materials<sup>11</sup>, which have been used to produce ‘unfeability cloaks’ (REF. 13). By layering different extremal materials, metamaterials with any desired  $C_{ijkl}$  can be created<sup>10</sup>.

**Heterogeneity.** The fundamental reason why architecting materials leads to new properties is the resulting heterogeneity of stresses and deformations, which causes the breakdown of the affine assumption, which conjectures that deformations are uniform, as in a homogeneous rubber sample<sup>76</sup>.

For example, for auxetic and extremal metamaterials most deformations are localized at the hinges, such that the global response of the material is entirely different from the local behaviour of its constituents. Such qualitative differences between the constituents and the collective are crucial for a wide variety of heterogeneous, structured media, such as foams<sup>77</sup>, granular media<sup>78</sup>, fibrous materials<sup>79</sup> and random spring networks<sup>80–83</sup>. For example, loosely connected networks of linear springs have a much smaller elastic response than that expected from a dimensional argument estimating the elastic modulus from the spring constant and characteristic length. In particular, the elastic response vanishes at a critical but finite value of the connectivity, for which the network is strongly nonaffine<sup>75,80–83</sup>. This dependence of the bulk elastic properties on the geometry of the network enables the design of geometries that result in specific elastic properties. By mimicking the geometry of jammed particle packings, networks with a vanishing shear-to-bulk modulus ratio can be obtained<sup>82</sup>, whereas targeted spring pruning has been used to achieve auxetic random spring networks with a diverging shear-to-bulk modulus ratio<sup>84</sup>. In all cases, subtle changes in the geometry of the disordered networks lead to qualitatively different deformations and elastic properties, which illustrates that the relation between the architecture and collective properties is rich and complex.

**Mechanism-based metamaterials**

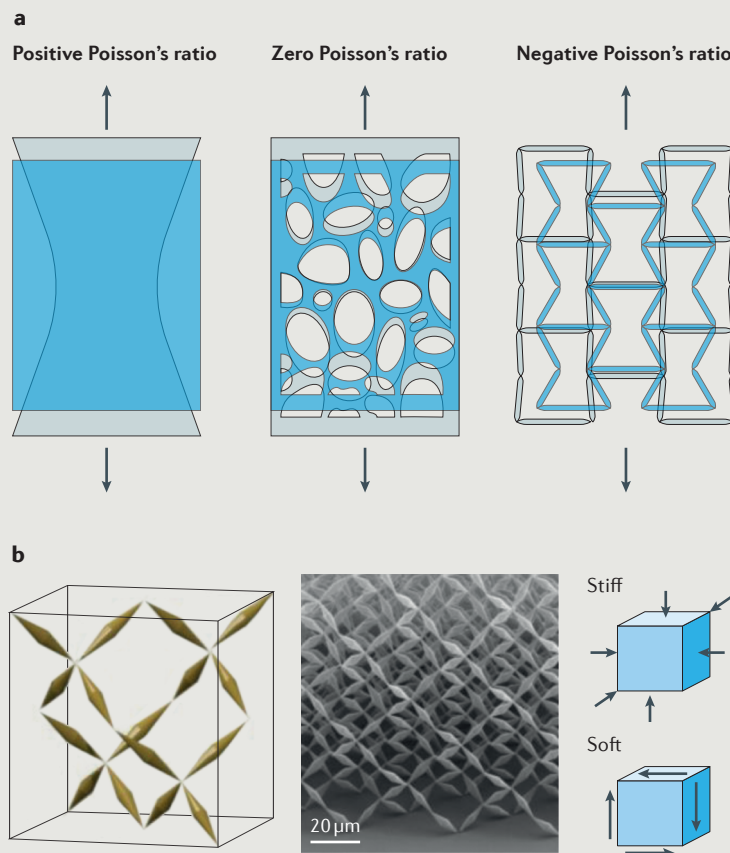
Mechanisms are collections of rigid elements linked by flexible hinges that have a geometric design that allows for a zero-energy, free motion. The designability of arbitrarily complex motions by careful choice of the geometry of the linked elements<sup>85</sup> makes mechanisms central to a wide range of engineering structures (such as levers, pulleys, linkages and gears), as well as a popular target for [shape-transforming art](#). Mechanisms also underlie a wide variety of mechanical metamaterials (FIG. 2). For example, a collection of squares linked at their tips form an auxetic structure (FIG. 2a), as they can undergo a free hinging motion that causes the structure to uniformly contract or expand. This design has inspired a range of soft metamaterials, as discussed below<sup>17,62,66,86–88</sup>. Plates linked by flexible hinges form origami metamaterials. The so-called Miura-ori structure (FIG. 2b), which was originally

## Box 1 | Auxetic and extremal metamaterials

**Auxetic metamaterials.** The application of a uniaxial stretch usually results in a lateral contraction (for example, a stretched rubber band becomes thinner in the transverse direction); thus, in this case, the ratio between transverse and axial strain, Poisson's ratio,  $\nu$ , is positive. For incompressible bulk materials, such as rubber,  $\nu$  is roughly  $\frac{1}{2}$ , but if a rubber sheet is patterned with a random arrangement of holes, the effective value of  $\nu$  approaches zero: although individual rubber filaments get thinner, the overall rubber/vacuum composite assembly does not. This is how random cellular solids, such as cork, achieve near-zero Poisson's ratios, which makes cork a practical material to seal wine bottles, as the cork does not expand laterally when inserted into the bottle by compressive forces. It is also possible to design patterns, such as the inverted hexagon pattern<sup>7,100</sup>, that result in auxetic metamaterials, that is, materials with a negative Poisson's ratio, even though the constituent material, rubber, has a positive Poisson's ratio. These examples show that appropriately designed architectures can push the properties of metamaterials beyond those of their constituents. In panel **a** of the figure, a rubber sheet, a random cellular material and an auxetic metamaterial are shown before (blue) and after (grey) the application of a longitudinal stretch.

**Extremal metamaterials.** Metamaterials that are designed to resist one particular mode of deformation are called extremal metamaterials<sup>10</sup>. Pin-jointed and inverted honeycomb lattices are examples of 2D extremal materials<sup>10</sup>. Panel **b** of the figure shows the theoretical unit cell and the experimental realization of a 3D extremal metamaterial that resists isotropic compression but is very soft against shear; in the limit of vanishingly small tips, which approach the limit of ideal hinges, the ratio of shear-to-bulk modulus approaches zero, and the response of the material becomes similar to that of a fluid.

Panel **b** is adapted with permission from REF. 11, American Institute of Physics.



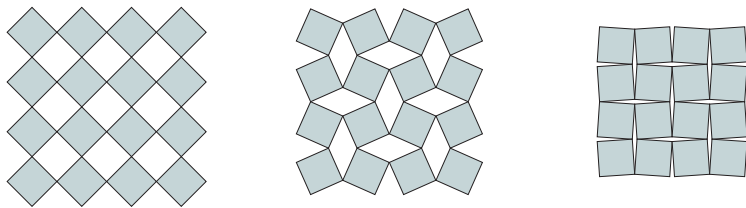
designed to obtain deployable solar panels for applications in space<sup>19</sup>, constitutes the starting point for a range of more complex shape-shifting and programmable origami metamaterials<sup>14,15,19–25,27,29,32,32,34,68,71,89–91</sup>. Finally, an asymmetric mechanism consisting of linked bars that allows motions to propagate from the right edge to the left edge but not vice versa was recently demonstrated; this is a prime example of a topological mechanical metamaterial<sup>37,38</sup> (FIG. 2c).

**Origami-based metamaterials.** The aesthetically pleasant patterns and shapes enabled by origami (from the Japanese words 'ori', meaning 'to fold', and 'kami', meaning 'paper') and kirigami (from 'kiru', 'to cut', and 'kami', 'paper') have long been admired, and origami-inspired geometries have been used to obtain deployable structures<sup>19</sup>, flexible medical stents<sup>89</sup> and flexible electronic devices<sup>90</sup>. Origami also provides a powerful platform for designing mechanism-based metamaterials, starting from 2D sheets with predefined crease patterns, such as the Miura-ori structure and its variants<sup>19,22,23,27,32,68</sup>, the square twist<sup>71</sup> and the box-pleat tiling<sup>20</sup> (FIG. 3). These 'metasheets' can serve as auxetic metamaterials<sup>14,22</sup> or be smoothly modified to fold into arbitrary shapes<sup>32</sup>. As origami-based mechanisms often feature multiple discrete folding motions, with only one continuous degree of freedom,

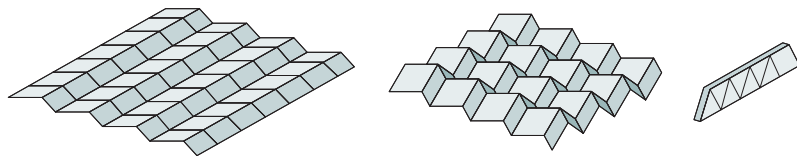
they enable the design of multishape metamaterials<sup>27</sup>. Moreover, exploring the competition between bending and hinging energies<sup>24,71</sup> allows the design of multistable and programmable materials<sup>27,32,68,71</sup>. Finally, fully 3D cellular metamaterials can be designed by stacking folded layers<sup>14</sup> and assembling them in tubes<sup>15,21,25,29</sup> (FIG. 3a), or by drawing inspiration from snapology<sup>34,35,91</sup>, a modular origami technique (FIG. 3b).

**Kirigami.** Kirigami-inspired metamaterials are produced by introducing arrays of cuts into thin sheets of a material (FIG. 3c). This allows the control of the elastic properties of the material<sup>31</sup> and the achievement of extremely large strains and shape changes<sup>16,26</sup>. The kirigami design principle has been exploited to transform one-atom-thick graphene sheets into resilient and movable structures<sup>92</sup>, to engineer elasticity in stiff (almost rigid) nanocomposites without compromising their electrical conductance<sup>28</sup>, and to design stretchable lithium-ion batteries<sup>93</sup> and diffraction gratings with tunable periodicity<sup>94</sup>. Furthermore, kirigami-patterned sheets exhibit out-of-plane deformations, which provides a route to form complex 3D mesostructures<sup>72,95</sup> and enables planar solar tracking<sup>96</sup>. Finally, by combining origami and kirigami, the design space can be greatly expanded<sup>97</sup> and complex surfaces can be realized<sup>98</sup>.

**a Auxetic metamaterial**



**b Origami-inspired metamaterial**



**c Topological metamaterial**

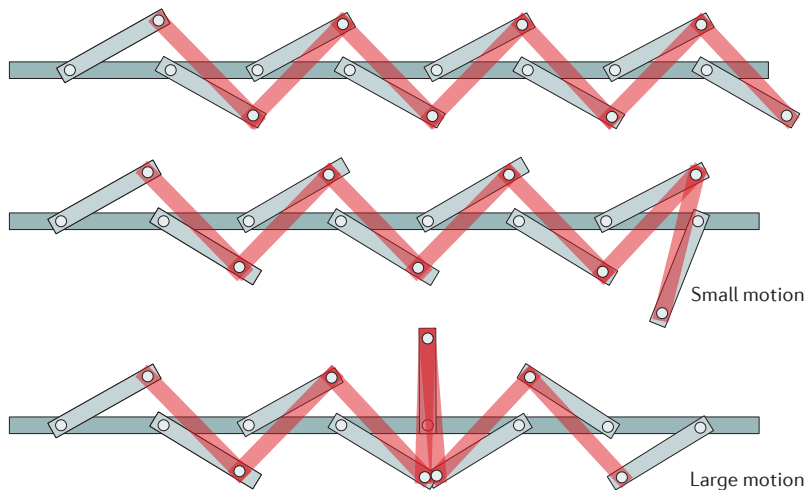


Figure 2 | **Mechanism-based metamaterials.** **a** | A collection of squares linked at their tips can undergo a volume-changing shape transformation; thus, it constitutes an auxetic mechanism<sup>86</sup>. **b** | Rigid plates linked by flexible hinges are the basis of origami metamaterials. The Miura-ori pattern shown here is a rigidly foldable origami mechanism with one degree of freedom<sup>19,22</sup>. **c** | Flexibly linked, rigid bars form a topologically polarized mechanism. A small motion of the first bar on the right remains localized near the right edge, whereas a larger motion initiates a domain wall that propagates to the left. By contrast, the leftmost bar cannot be moved; thus, propagation to the right is not possible<sup>37,38</sup>.

**Soft mechanism-based metamaterials.** The geometric design of mechanisms can also be used to create soft mechanism-based metamaterials that have slender, flexible parts as hinges, connecting stiffer elements that can easily rotate. The low-energy deformations of these metamaterials closely shadow the free motion of the underlying mechanism. External forces easily excite these soft modes, which generally have a specific spatial structure, very different from the smooth deformations of ordinary elastic media. This allows the design of soft metamaterials that undergo programmable shape shifting, ranging from 2D (REFS 62,66,86–88) and 3D (REFS 17,30,99) auxetic materials to size-morphing spheres that can be used as reversible encapsulation systems<sup>64</sup> (FIG. 4a). Moreover, by using combinatorial techniques to connect different

unit cells, it was recently shown that aperiodic mechanical metamaterials that exhibit precisely pre-programmable shape changes can be rationally designed<sup>30</sup> (FIG. 4b). In all these examples, as mentioned, the hinges are slender beams; as discussed in the next section, this can be exploited to produce nonlinear, collective buckling phenomena under compression.

**Instability-based metamaterials**

Elastic instabilities and large deformations enable the achievement of strongly nonlinear relations between macroscopic stresses and strains, even if the material remains in the near-linear regime. Hence, various mechanical metamaterials are made of meta-atoms that give access to these nonlinearities. Slender elements can create large deformations in response to small forces, which leads to so-called geometric nonlinearities. Symmetric slender elements can undergo buckling instabilities that result in strong but reversible nonlinearities under precisely designable loading conditions. Finally, many elastic structures feature two stable states connected by a rapid and irreversible ‘snap-through’ instability (FIG. 1). Creating mechanical metamaterials by assembling these nonlinear and multistable building blocks leads to a range of completely new functionalities.

**Buckling-based metamaterials.** Highly porous materials consisting of networks of beams are ubiquitous in nature and in synthetic structures and devices<sup>100</sup>. Their functionality depends on both the deformation mechanism of the ligaments, which buckle under compression at relatively low strains, and on their microscopic geometry. In disordered elasto-plastic porous materials, buckling of the beam-like ligaments results in irreversible deformations in the form of collapse bands that provide an efficient energy-absorbing mechanism<sup>101–105</sup>. In metamaterials composed of regular arrays of elastic beams, buckling may trigger dramatic homogeneous and reversible pattern transformations. The simplest example of such a buckling-based metamaterial is a square array of circular holes embedded in an elastomeric sheet<sup>62,63,106</sup> (FIG. 5a), which can be seen as an array of rigid domains connected by beams. When the structure is uniaxially compressed, buckling of the beam-like ligaments triggers a sudden transformation of the holes into a periodic pattern of alternating and mutually orthogonal ellipses. Thus, this metamaterial combines the shape-transforming properties of the underlying mechanism of hinged squares with the mechanical functionality of the beam elements that connect these square elements.

For elastic materials, the geometric reorganization triggered by the instability is both reversible and repeatable. Furthermore, it occurs over a narrow range of applied loads, which makes it promising for the creation of materials with properties that can switch in a sudden but controlled manner. This parallel and cooperative buckling, leading to a predictable transformation between different microstructures, is instrumental for the design of materials with tunable properties, including systems with a tunable negative Poisson’s ratio<sup>63,107</sup> and an effective negative swelling ratio<sup>18</sup>, phononic<sup>108–110</sup>



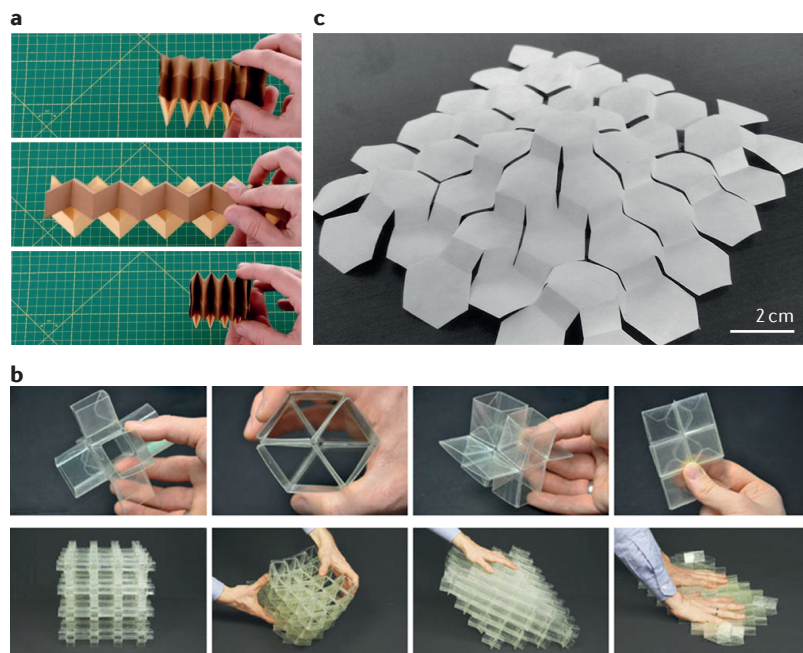


**Figure 3 | Origami-inspired metamaterials.** **a** | Deployment and retraction of a 'zipper'-coupled tube system<sup>29</sup>. This origami has only one flexible motion through which it can deform and is very stiff against other deformations. The structure is lightweight and can be deployed by acting only on its right end. **b** | Inspired by snapology, a type of modular origami, a highly flexible mechanical metamaterial with a cubic microstructure was designed; this metamaterial allows for a number of well-defined shape changes and can be folded flat<sup>34</sup>. **c** | Combining origami and kirigami, that is, using both cuts and folds, allows the easy formation of arbitrary 3D objects starting from 2D sheets<sup>98</sup>. Panel **a** is adapted with permission from REF. 29, National Academy of Sciences. Panel **b** is adapted with permission from REF. 34, Macmillan Publishers Limited. Panel **c** is adapted with permission from REF. 98, National Academy of Sciences.

and photonic<sup>111</sup> switches and colour displays<sup>112</sup>, and systems with switchable chirality<sup>113</sup>. By breaking the symmetry of the undeformed pattern, that is, by substituting circular holes with elliptical holes, the sharp buckling transformation is smeared out, leading to a tunable nonlinearity of the effective constitutive law, which has been leveraged to control the buckling behaviour of metabeams (which are beams made of a mechanical metamaterial)<sup>66</sup>. In all these examples, the structures recover their initial shape when unloaded.

**Snapping-based instabilities.** Elastic beams may also snap between two different stable configurations, retaining their deformed shape after unloading<sup>67,114,115</sup>. As bistable elastic beams can lock in most of the energy provided to the system during loading, they have been recently used to create fully elastic and reusable energy-trapping metamaterials<sup>33,70,116</sup> (FIG. 5b). Moreover, the ability of bistable beams to release stored elastic energy has been exploited to overcome both dissipative and dispersive effects to allow the propagation of mechanical signals with a large amplitude in soft systems made of dissipative materials<sup>73</sup>. Finally, whereas most instability-based metamaterials work only under compressive loadings, a mechanical metamaterial composed of a periodic arrangement of snapping units (consisting of two curved parallel beams that are centrally clamped)

undergoes a large extension under tension caused by sequential snap-through instabilities. The material also exhibits a pattern switch from a wavy shape to a diamond configuration<sup>74</sup>.

**Frustrated and programmable metamaterials.** An important consideration in the design of metamaterials is whether all building blocks should be able to deform cooperatively, that is, whether the metamaterial should be frustration-free. In general, frustration leads to a complex energy landscape with a plethora of energy minima, which can hinder any desired functionality. However, a controlled amount of frustration can be leveraged to obtain multistable and programmable behaviour. Perhaps the simplest examples are the deformations of flexible origami metamaterials — obtained by 'popping through' some of the folds — which have been used to obtain a programmable stiffness<sup>68</sup> (FIG. 6a). Moreover, incompatible folding patterns for which folding necessitates plate bending can be used to obtain a programmable and multistable response<sup>32,71</sup>.

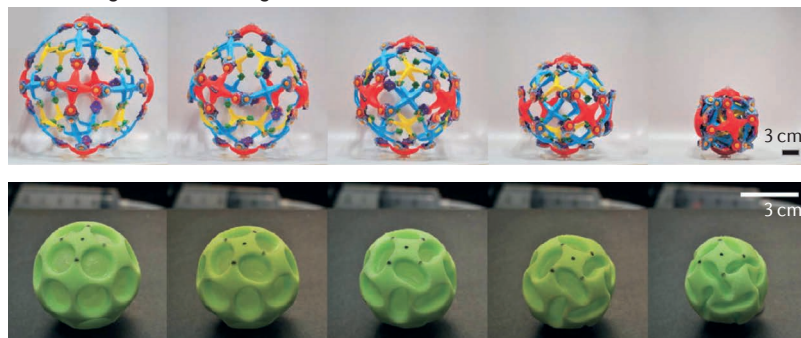
To achieve frustration-free operation in beam networks, all elastic elements should buckle into the most energetically favoured configuration (a half sinusoid) while preserving the angles with their neighbours to minimize the deformation energy. In two dimensions this requirement can be easily satisfied on a square lattice, but not on a triangular lattice, so that the system becomes frustrated and favours the formation of complex ordered patterns<sup>69</sup> (FIG. 6b). More generally, meta-atoms that leverage instabilities and geometric nonlinearities to become bistable or multistable can lead to tunable or programmable metamaterials that adapt their functionality depending on the configuration of their building blocks. For example, an inhomogeneous confinement applied to a biholar metamaterial creates a competition between two micropatterns; this effect has been exploited to realize a complex multistable system with a programmable response<sup>65</sup> (FIG. 6c). Finally, subjecting a shape-morphing metamaterial to incompatible boundary conditions can yield a response that depends non-trivially on the texture of both the material and the boundaries<sup>30</sup>.

### Topological metamaterials

Topological mechanical metamaterials display properties that are topologically protected. The properties of non-topological metamaterials are sensitive to both random and systematic changes in their microstructure. By contrast, topologically protected properties are not affected by smooth deformations of the underlying geometry or by the presence of disorder. Therefore, topological metamaterials provide an exciting pathway towards materials with robust functionalities.

The concept of topological protection is a hallmark of modern condensed matter physics and has a crucial role in quantum Hall systems and electronic topological insulators<sup>117</sup>. Like their counterparts in electronics and photonics, topological mechanical systems can have classical states (such as free motions, load-bearing states or vibrations), the existence of which is directly linked to the presence of a topological index<sup>36–60</sup>. Topological indices

**a Buckling-induced folding**



**b Metacube obtained with a combinatorial approach**

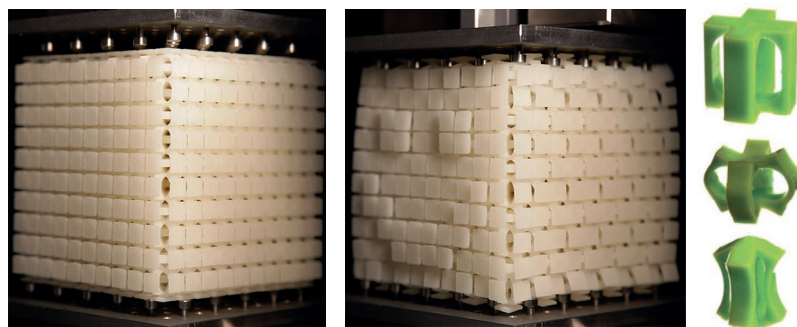


**Figure 4 | Mechanism-based, shape-morphing metamaterials.** **a** | The Hoberman Twist-O (top) is a commercial toy composed of a rigid network of struts connected by rotating hinges. It can easily collapse into a ball measuring a fraction of its original size. This structure is a mechanism because it has a single continuous degree of freedom. The buckliball (bottom), a structure created by researchers at the Massachusetts Institute of Technology, is inspired by this popular toy but applies the mechanism design to an elastic spherical shell. Under pneumatic actuation, the buckliball undergoes buckling-induced folding, opening avenues for a new class of active and reversible encapsulation systems<sup>64</sup>. **b** | A cubic unit cell with a single soft mode can deform into two different shapes that fit together in several ways. A combinatorial approach enables the design of a metacube consisting of  $10 \times 10 \times 10$  unit cells, each oriented differently in such a way that under uniaxial compression, a patterned texture appears on one of the faces of the metacube (surface pedestals are added to aid the visualization of the texture)<sup>30</sup>. Panel **a** is adapted with permission from REF. 64, National Academy of Sciences. Panel **b** is adapted with permission from REF. 30, Macmillan Publishers Limited.

are typically integer-valued quantities that cannot be changed by continuous deformations of the underlying structure<sup>117</sup>. A simple example is the genus of a surface, which denotes the number of holes in the surface; from the perspective of topology, a doughnut and a tea cup are equivalent, because the two shapes can be smoothly deformed into one another without introducing cuts. In topological metamaterials, the topological indices do not characterize the structures themselves, but rather their excitations, such as vibrational modes or elastic waves.

**Topological mechanisms and states of self-stress.** The simplest topological metamaterials are mechanisms that display a peculiar breaking of inversion symmetry. An example is a structure composed of a chain of rigid rotors connected by rigid beams<sup>37,38</sup> (FIG. 2c). To understand the properties of this linkage (and of many other mechanical structures), it is useful to view them as networks composed of  $N_s$  sites (such as point masses) connected by  $N_b$  central force bonds (such as springs or

rigid beams). In  $d$  dimensions, the number of degrees of freedom is given by  $dN_s$ , and the total number of constraints is simply  $N_b$ . The number of zero-energy modes  $n_m$ , which are soft deformations that at the lowest order cost no energy, is then given by the Maxwell criterion<sup>118</sup>

$$dN_s - N_b = n_m - n_{ss} \quad (2)$$

where  $n_{ss}$  denotes the number of redundant constraints or, equivalently, the number of states of self-stress, which are tensions or compressions applied to the bonds that do not result in net forces on the nodes.

Breaking the left–right symmetry of the unit cell can induce topological polarization, a concept we discuss in more detail later in this section<sup>38</sup>. Put simply, as an electrically polarized material can host localized charges at opposite boundaries, a topologically polarized material can have zero modes or states of self-stress at its edges. For example, in a topological chain composed of rigid bars and springs (FIG. 7a), the orientation and length of the bars determines the extension of the springs. Assuming that the springs are neither stretched nor compressed, there is a zero-energy deformation that satisfies the linearized constraint equation  $bu_{n+1} - au_n = 0$ , where  $u_n$  is the horizontal displacement of the  $n^{\text{th}}$  node connecting adjacent bars and springs, and  $a$  and  $b$  are structural parameters characteristic of the geometry of the unit cell<sup>37,38</sup>. Solving this equation yields  $u_{n+1} = (a/b)u_n$ . Thus, depending on whether  $a/b$  is greater or less than one, displacements are amplified or reduced, respectively. Equivalently, a floppy mode (a zero-energy mode) is localized near the right ( $a > b$ ) or left ( $a < b$ ) edge of the chain, depending on which of the two directions the bars lean, and the topological polarization points to the right or left, respectively.

In this example, there are no redundant constraints. In the absence of boundaries (for example, on a closed ring), this system has as many degrees of freedom (the angles of the rotors) as constraints (the number of beams) and no zero modes. However, for a finite chain (obtained by cutting the ring), one constraint is missing and a zero-energy mode appears in the system; there is no linear restoring force that stops this motion. The Maxwell criterion does not prescribe where this zero mode is located, but a more detailed calculation using the dynamical matrix reveals that the zero-energy eigenmode is localized at the edge towards which the rotors point<sup>37</sup>.

This zero mode requires a system with edges, but its location reflects the breaking of the inversion symmetry of the unit cell, which is a bulk property linked to a topological index in the vibrational spectrum<sup>37</sup>. Intriguingly, these localized zero-energy modes can be moved anywhere in the system by exploiting the nonlinear domain walls that reconfigure the structure without stretching any of the beams<sup>38</sup> (FIG. 2c). Smooth deformations of the network leave the left side of equation 2 unchanged; this means that after such a smooth deformation, the difference between the number of zero modes and states of self-stress remains invariant, even if  $n_m$  and  $n_{ss}$  change. The condition  $dN_s - N_b = 0$  can be viewed as a charge neutrality condition, with the roles of positive and



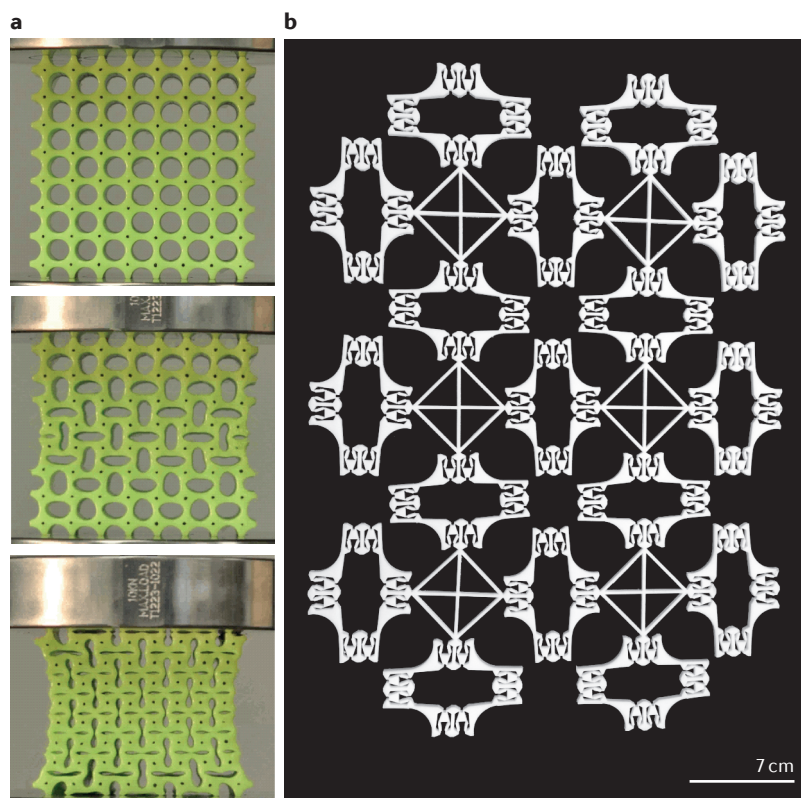


**Figure 5 | Instability-based metamaterials.** **a** | A rubber slab patterned with circular holes undergoes a reversible pattern transformation when compressed as a result of a collective buckling-like instability<sup>62,63,106</sup>. **b** | A reconfigurable metamaterial containing complex hinge units that provide multiple kinematic degrees of freedom and multistability<sup>33</sup>. Panel **a** is adapted with permission from REF. 87, Wiley-VCH. Panel **b** is adapted with permission from REF. 33, Wiley-VCH.

negative charge played by the zero modes and states of self-stress. The crucial point is that the existence of the zero mode is topologically protected, that is, it persists for a wide range of smooth structural deformations, such as small changes in beam length<sup>119</sup>.

In the following, we focus our attention on periodic mechanical structures that are ‘charge neutral’ but mechanically polarized, so that edge modes can appear at the sample boundary like charges in an electrically polarized medium. This mechanical polarization is defined in terms of topological invariants of the bulk structure<sup>37</sup>. Just as Gauss’s law yields the net electric charge enclosed in a region from the flux of the electric polarization through its boundary, the difference between the number of topological zero modes (the modes that arise without adding or removing bonds anywhere in the structure) minus the number of topological states of self-stress in an arbitrary portion of an isostatic lattice is given by the flux of the topological polarization through its boundary<sup>37</sup>. Thus, domain walls between regions of different polarization can localize zero modes or states of self-stress inside a material as well as at its edges (examples of macroscopic prototypes are shown in FIG. 7). These principles have been used to create stable geared topological metamaterials with protected edge and bulk states<sup>45</sup> (FIG. 7b), to develop topological origami that folds more easily

from one side<sup>48</sup> (FIG. 7c), to elucidate how dislocations can localize topological zero modes and states of self-stress<sup>40</sup> (FIG. 7d), to produce transformable metamaterials that can switch their topological polarization<sup>51</sup> (FIG. 7e), to generate nonreciprocal mechanical metamaterials analogous to acoustic diodes<sup>61</sup> and to demonstrate topological control of buckling via states of self-stress in 3D cellular metamaterials<sup>41</sup> (FIG. 7f). The last example shows that states of self-stress are related to the propensity of the structure to locally respond to stress focusing with mechanical failure, in the same way as zero modes can be set in motion if externally activated.

**Topological waves.** In addition to zero-frequency topological modes, topologically protected modes can also occur at finite frequencies, including those involved in mechanical waves. An example is the propagation of mechanical waves in the lattices of either coupled gyroscopes<sup>42,59</sup> or pendula<sup>53</sup> (FIG. 7g,h). The phononic band structure of these systems exhibits gaps — frequency ranges in which mechanical waves cannot propagate in the bulk. However, in a finite sample, these gaps are populated by waves that can propagate only at the sample edge. These phononic edge states are topologically protected in the sense that the waves do not scatter if the shape of the boundary changes (even in the presence of sharp corners, as in FIG. 7h) or if disorder is present<sup>120</sup>.

The phonon localization at the edge is not caused by local variations in material parameters at the boundary. Instead, it is a manifestation of a general and deep physical principle known as the bulk–edge correspondence<sup>117</sup>, which is also at the base of the localization of the zero modes, as shown in FIG. 7a. The phononic band structure of these metamaterials is characterized by the presence of integer-valued topological invariants, the Chern numbers. The Chern number abruptly changes at the sample edge, which separates the topological from the normal medium; for the Chern number to change, a gap closing must occur. Thus, as a result of the topological nature of the bulk band structure, gapless edge modes appear, irrespective of the boundary shape.

This mechanism is common to all topological metamaterials (as well as to several classes of electronic and photonic topological insulators). Different physical mechanisms may be responsible for the opening of the gaps in the band structure. For example, in gyroscopic lattices<sup>42,59</sup> and in proposed metamaterials based on rotating fluids<sup>43,52,121</sup>, the gap arises from the breaking of the time-reversal symmetry. As a result, wave propagation at the edge is unidirectional and immune to backscattering. The propagation direction of the edge mode is determined by the interplay between the sense of rotation of the microscopic degrees of freedom (gyroscopes or annuli filled with rotating fluids) and the geometry of the lattice. Particularly exciting is the prospect of self-assembling mechanical topological insulators based on active liquids that flow spontaneously without external drive in confined geometries<sup>121</sup>. The underlying active chiral flow would break time-reversal symmetry, giving rise to robust unidirectional acoustic waveguides at the sample edges and domain walls.

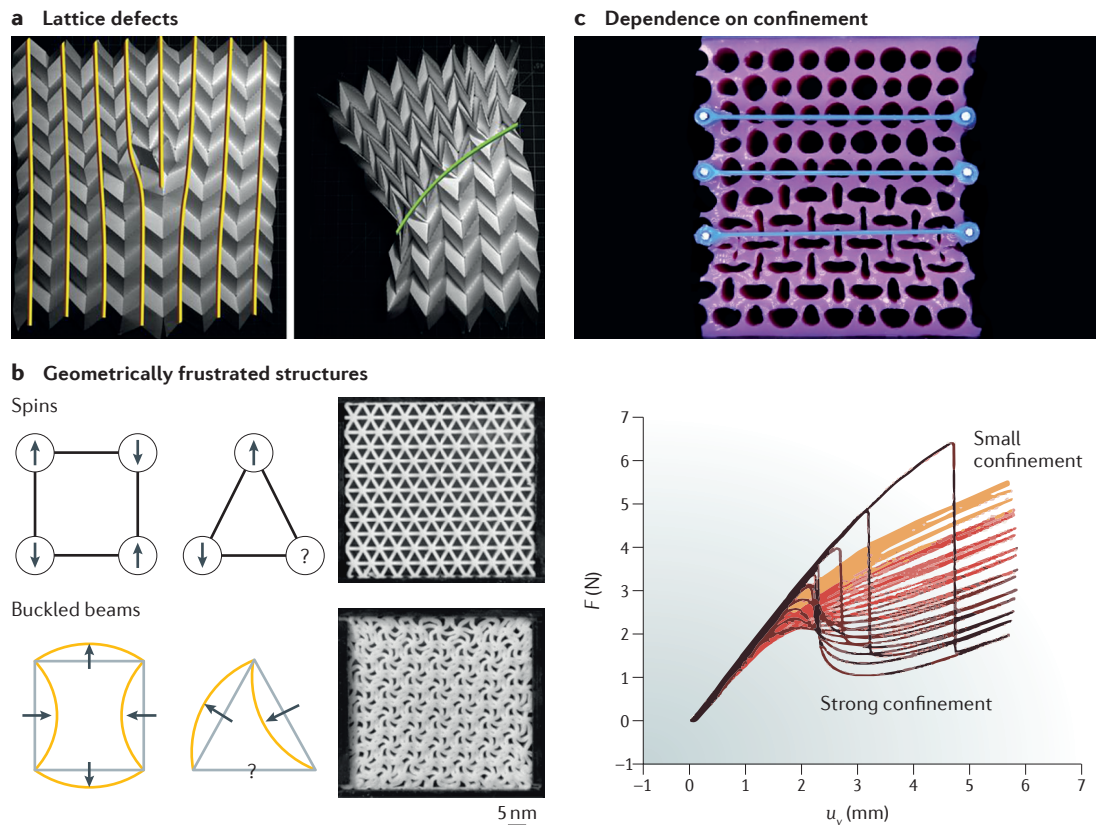


**Figure 6 | Frustration and tunable metamaterials.** **a** | Each unit cell of the Miura-ori tessellation is mechanically bistable. By switching between states, that is, by locally ‘popping through’ the fold pattern, the compressive modulus of the overall structure can be rationally and reversibly tuned. By virtue of their interactions, these mechanically stable lattice defects also lead to emergent crystallographic structures, such as vacancies, dislocations (left) and grain boundaries (right)<sup>68</sup>. **b** | Similar to how spins can order or assume a frustrated configuration depending on the symmetry of the underlying lattice, buckled beams on frames tend to preserve the angles at joints to minimize the deformation energy. This can be realized for square frames but not for triangular frames, leading to frustration. In geometrically frustrated cellular structures, buckling triggered under equibiaxial compression results in the formation of complex ordered patterns<sup>69</sup>. **c** | In a metamaterial with alternating large and small holes, competition between two differently buckled patterns arises if horizontal confinement is introduced (blue bars). As shown in the plot, the vertical force  $F$  as function of the vertical compression  $u_y$  depends on the degree of confinement. For small confinement, the mechanical response is monotonic, whereas for increasingly strong confinement, the response becomes nonmonotonic and eventually displays hysteresis; confinement can thus be used to programme the mechanical response of a metamaterial<sup>65</sup>. Panel **a** is adapted with permission from REF. 68, AAAS. Panel **b** is adapted with permission from REF. 69, American Physical Society.

## Outlook

Fuelled by rapid advances in additive manufacturing, computational design and conceptual breakthroughs, research in mechanical metamaterials is bringing about many exciting developments. We close this Review by identifying several challenges for future work.

First, most studies so far have focused on small, pristine samples, but new phenomena will arise in larger samples. Although it is often tacitly assumed that deformations in mechanical metamaterials are essentially homogeneous and follow an idealized design, in practice, a finite and perhaps large correlation length is expected, beyond which gradients, domain walls or grain boundaries may arise<sup>122</sup>. Moreover, defects often dominate or alter the material behaviour, and it is an open question how defects, either resulting from fabrication errors or purposely introduced<sup>40,68</sup>, change the properties of mechanical metamaterials.

Second, although many mechanical metamaterials are composed of periodic structures, more advanced, spatially textured functionalities require aperiodic materials. The design of spatially textured metastructures has advanced substantially for origami-based metamaterials; for these structures, computer software, such as TreeMaker, can generate folding patterns that allow the transformation of flat sheets into arbitrary 3D shapes<sup>123</sup> and perturbative techniques that create folding patterns that approach arbitrary, smooth 3D surfaces have recently been introduced<sup>32</sup>. For other types of mechanical metamaterials, such techniques are generally not available, although a combinatorial strategy for the rational design of aperiodic, yet frustration-free, shape-shifting metamaterials has recently been introduced<sup>30</sup>. Much more work is needed to develop these notions into a coherent framework, and many questions remain open. For example, it is not yet clear how to design metamaterials



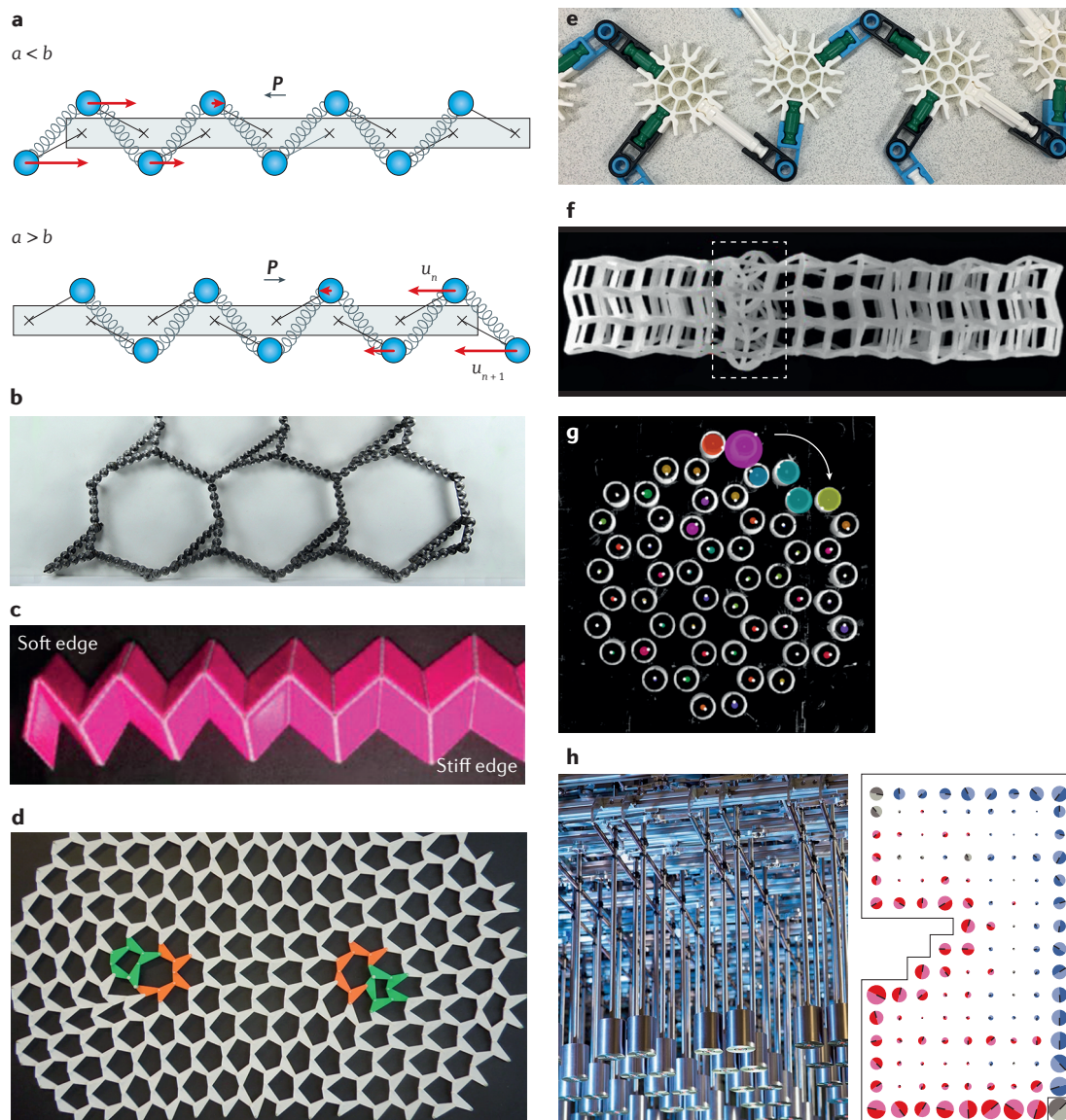


Figure 7 | **Prototypes of topological mechanical metamaterials.** **a** | A topological chain composed of rigid bars and springs. Depending on the parameters of the system,  $a$  and  $b$ , a floppy mode is localized either at the right or at the left side of the chain. The topological polarization  $P$  is indicated as well as the displacements  $u_n$  and  $u_{n+1}$  (red arrows). **b** | Gears mounted on solid links, connected through joints and arranged into a lattice to form a geared topological metamaterial<sup>45</sup>. **c** | Topological origami<sup>48</sup>. **d** | Zero mode localized at a dislocation on the left of the topological metamaterial and corresponding state of self-stress localized at a dislocation on the right<sup>40</sup>. **e** | Detail of a metamaterial that can switch its topological polarization<sup>51</sup>. **f** | Topological state of self-stress localized at a domain wall; under compression, stresses concentrate here, leading to selective buckling<sup>41</sup>. **g** | Gyroscoptic metamaterial that supports topologically protected chiral edge states — the false colours represent the phase of a snapshot of a chiral edge wave<sup>42</sup>. **h** | A system of suitably coupled pendula (left) provides a mechanical analogue of the quantum spin Hall effect and hosts topologically protected acoustic waveguides at its edge (right); the blue and red circles represent the polarization of the chiral edge waves<sup>44</sup>. Panel **b** is adapted from REF. 45 under a Creative Commons license [CC BY 3.0](https://creativecommons.org/licenses/by/3.0/). Panel **c** is adapted with permission from REF. 48, American Physical Society. Panel **d** is adapted with permission from REF. 40, Macmillan Publishers Limited. Panel **e** is adapted with permission from REF. 51, Macmillan Publishers Limited. Panel **f** is adapted with permission from REF. 41, National Academy of Sciences. Panel **g** is adapted with permission from REF. 42, National Academy of Sciences. Panel **h** (left) is courtesy of H. Hostettler, ETH Zürich, Switzerland. Panel **h** (right) is adapted with permission from REF. 44, AAAS.

that can morph into a distinct number of predefined shapes.

Third, more complex metamaterials that explore complex energy landscapes and activities are on the horizon. Several examples of frustrated metamaterials

that feature multistability and programmability have been recently demonstrated<sup>27,30,65,69</sup>. Rational design of the underlying complex energy landscapes is still in its infancy but would allow the creation of a host of more complex metamaterials, potentially leading to

functionalities such as information storage and retrieval, which are prerequisites for more complex programmable materials. If activated by motors or external fields, shape-shifting metamaterials can be used to create useful robotic structures<sup>124</sup>. The deep integration of actuation and the amplification of mechanical information are crucial to overcome the inevitable dissipative processes, and if combined with information processing (for example, using logic gates<sup>73</sup>) would open the door to truly smart metamaterials.

Fourth, additive manufacturing techniques, from 3D printing to laser cutting and two-photon lithography, have played a crucial part in enabling the shaping and patterning of mechanical metamaterials. Many of these techniques are still in their early stages, and the range of base materials that can be printed is still limited. Combining multiple (contrasting) materials is very challenging, but the ability to mix elastic, plastic and viscous materials could lead to completely new classes of mechanical meta-behaviours. Moreover, the inclusion of materials that have specific functionalities may enable hybrid — for example, opto-mechanical, thermo-mechanical or electro-mechanical — classes of metamaterials.

Fifth, the range of scales and aspect ratios that can be achieved currently is limited. Combinations of top-down and bottom-up (self-assembly) techniques may allow the translation of metamaterial concepts to smaller scales, for example, by combining graphene origami<sup>92</sup>, colloidal self-assembly<sup>125</sup> and even chemistry to create designer materials sculpted over a wide range of scales.

Finally, the rational design of metamaterials with a target property or functionality remains fiendishly difficult, and many designs so far have relied on luck and intuition. For example, Kempe's universality theorem states that it is possible to construct a pantograph-type mechanism that traces out any desired complex motion; however, in all but the simplest cases, the mathematics produces such complex linkages that the practical applicability of this theorem is limited<sup>85</sup>. We expect that a combination of rational and combinatorial techniques and topological concepts with computer-aided design techniques, such as evolutionary algorithms<sup>126</sup>, will increasingly allow researchers to create mechanical metamaterials with more complex and targeted functionalities.

1. Soukoulis, C. & Wegener, M. Past achievements and future challenges in the development of three-dimensional photonic metamaterials. *Nat. Photonics* **5**, 523–530 (2011).
2. Cummer, S. A., Christensen, J. & Alù, A. Controlling sound with acoustic metamaterials. *Nat. Rev. Mater.* **1**, 16001 (2016).
3. Schittny, R., Kadic, M., Guenneau, S. & Wegener, M. Experiments on transformation thermodynamics: molding the flow of heat. *Phys. Rev. Lett.* **110**, 195901 (2013).
4. Pendry, J. B. Negative refraction makes a perfect lens. *Phys. Rev. Lett.* **85**, 3966–3969 (2000).
5. Kadic, M., Bückmann, T., Schittny, R. & Wegener, M. Metamaterials beyond electromagnetism. *Rep. Prog. Phys.* **76**, 126501 (2013).
6. Christensen, J., Kadic, M., Kraft, O. & Wegener, M. Vibrant times for mechanical metamaterials. *MRS Commun.* **5**, 453–462 (2015).
7. Lakes, R. Foam structures with a negative Poisson's ratio. *Science* **235**, 1038–1040 (1987).
8. Lakes, R. Deformation mechanisms of negative Poisson's ratio materials: structural aspects. *J. Mater. Sci.* **26**, 2287–2292 (1991).
9. Milton, G. Composite materials with poisson's ratios close to — 1. *J. Mech. Phys. Solids* **40**, 1105–1137 (1992).
10. Milton, G. W. & Cherkaev, A. V. Which elasticity tensors are realizable? *J. Eng. Mater. Technol.* **117**, 483–493 (1995).
11. Kadic, M., Bückmann, T., Stenger, N., Thiel, M. & Wegener, M. On the practicability of pentamode mechanical metamaterials. *Appl. Phys. Lett.* **100**, 191901 (2012).
12. Nicolaou, Z. G. & Motter, A. E. Mechanical metamaterials with negative compressibility transitions. *Nat. Mater.* **11**, 608–613 (2012).
13. Bückmann, T., Thiel, M., Kadic, M., Schittny, R. & Wegener, M. An elasto-mechanical unfeelability cloak made of pentamode metamaterials. *Nat. Commun.* **5**, 4130 (2014).
14. Schenk, M. & Guest, S. D. Geometry of miura-folded metamaterials. *Proc. Natl Acad. Sci. USA* **110**, 3276–3281 (2013).
15. Yasuda, H. & Yang, J. Reentrant origami-based metamaterials with negative Poisson's ratio and bistability. *Phys. Rev. Lett.* **114**, 185502 (2015).
16. Gatt, R. et al. Hierarchical auxetic mechanical metamaterials. *Sci. Rep.* **5**, 8395 (2015).
17. Babaei, S. et al. 3D soft metamaterials with negative Poisson's ratio. *Adv. Mater.* **25**, 5044–5049 (2013).
18. Liu, J. et al. Harnessing buckling to design architected materials that exhibit effective negative swelling. *Adv. Mater.* **28**, 6619–6624 (2016).
19. Miura, K. Method of packaging and deployment of large membranes in space. *Inst. Space Astronaut. Sci. Rep.* **618**, 1–9 (1985).
20. Hawkes, E. et al. Programmable matter by folding. *Proc. Natl Acad. Sci. USA* **107**, 12441–12445 (2010).
21. Tachi, T. & Miura, K. Rigid-foldable cylinders and cells. *J. Int. Shell Spat. Struct.* **53**, 217–226 (2012).
22. Wei, Z. Y., Guo, Z. V., Dudte, L., Liang, H. Y. & Mahadevan, L. Geometric mechanics of periodic pleated origami. *Phys. Rev. Lett.* **110**, 215501 (2013).
23. Lv, C., Krishnaraju, D., Konjevod, G., Yu, H. & Jiang, H. Origami based mechanical metamaterials. *Sci. Rep.* **4**, 5979 (2014).
24. Lechenault, F., Thiria, B. & Adda-Bedia, M. Mechanical response of a creased sheet. *Phys. Rev. Lett.* **112**, 244301 (2014).
25. Cheung, K. C., Tachi, T., Calisch, S. & Miura, K. Origami interleaved tube cellular materials. *Smart Mater. Struct.* **23**, 094012 (2014).
26. Cho, Y. et al. Engineering the shape and structure of materials by fractal cut. *Proc. Natl Acad. Sci. USA* **111**, 17390 (2014).
27. Waitukaitis, S., Menaut, R., Chen, B. G. & van Hecke, M. Origami multistability: from single vertices to metasheets. *Phys. Rev. Lett.* **114**, 055503 (2015).
28. Shyu, T. et al. A kirigami approach to engineering elasticity in nanocomposites through patterned defects. *Nat. Mater.* **14**, 785–789 (2015).
29. Filipov, E. T., Tachi, T. & Paulino, G. H. Origami tubes assembled into stiff, yet reconfigurable structures and metamaterials. *Proc. Natl Acad. Sci. USA* **112**, 12321–12326 (2015).
30. Coulais, C., Teomy, E., de Reus, K., Shokef, Y. & van Hecke, M. Combinatorial design of textured mechanical metamaterials. *Nature* **535**, 529–532 (2016).
31. Isobe, M. & Okumura, K. Initial rigid response and softening transition of highly stretchable kirigami sheet materials. *Sci. Rep.* **6**, 24758 (2016).
32. Dudte, L., Vouga, E., Tachi, T. & Mahadevan, L. Programming curvature using origami tessellations. *Nat. Mater.* **15**, 583–588 (2016).
33. Haghpanah, B. et al. Multistable shape-reconfigurable architected materials. *Adv. Mater.* **28**, 7915–7920 (2016).
34. Overvelde, J. T. et al. A three-dimensional actuated origami-inspired transformable metamaterial with multiple degrees of freedom. *Nat. Commun.* **7**, 10929 (2016).
35. Overvelde, J. T., Weaver, J., Hoberman, C. & Bertoldi, K. Rational design of reconfigurable prismatic architected materials. *Nature* **541**, 347–352 (2017).
36. Prodan, E. & Prodan, C. Topological phonon modes and their role in dynamic instability of microtubules. *Phys. Rev. Lett.* **103**, 248101 (2009).
37. Kane, C. L. & Lubensky, T. C. Topological boundary modes in isostatic lattices. *Nat. Phys.* **10**, 39–45 (2014).
38. Chen, B. G., Upadhyaya, N. & Vitelli, V. Nonlinear conduction via solitons in a topological mechanical insulator. *Proc. Natl Acad. Sci. USA* **111**, 13004–13009 (2014).
39. Vitelli, V., Upadhyaya, N. & Chen, B. G. Topological mechanisms as classical spinor fields. Preprint at <http://arxiv.org/abs/1407.2890v2> (2014).
40. Paulose, J., Chen, B. G. & Vitelli, V. Topological modes bound to dislocations in mechanical metamaterials. *Nat. Phys.* **11**, 153–156 (2015).
41. Paulose, J., Meeussen, A. S. & Vitelli, V. Selective buckling via states of self-stress in topological metamaterials. *Proc. Natl Acad. Sci. USA* **112**, 7639–7644 (2015).
42. Nash, L. M. et al. Topological mechanics of gyroscopic metamaterials. *Proc. Natl Acad. Sci. USA* **112**, 14495–14500 (2015).
43. Khanikaev, A. B., Fleury, R. & Mousavi, S. H. & Alù, A. Topologically robust sound propagation in an angular-momentum-biased graphene-like resonator lattice. *Nat. Commun.* **6**, 8260 (2015).
44. Susstrunk, R. & Huber, S. D. Observation of phononic helical edge states in a mechanical topological insulator. *Science* **349**, 47–50 (2015).
45. Meeussen, A. S., Paulose, J. & Vitelli, V. Geared topological metamaterials with tunable mechanical stability. *Phys. Rev. X* **6**, 041029 (2016).
46. Rocklin, D. Z., Chen, B. G., Falk, M., Vitelli, V. & Lubensky, T. C. Mechanical Weyl modes in topological Maxwell lattices. *Phys. Rev. Lett.* **116**, 135503 (2016).
47. Kariyado, T. & Hatsugai, Y. Manipulation of Dirac cones in mechanical graphene. *Sci. Rep.* **5**, 18107 (2015).
48. Chen, B. G. et al. Topological mechanics of origami and kirigami. *Phys. Rev. Lett.* **116**, 135501 (2016).
49. Mousavi, S. H., Khanikaev, A. B. & Wang, Z. Topologically protected elastic waves in phononic metamaterials. *Nat. Commun.* **6**, 8682 (2015).
50. Xiao, M., Chen, W.-J., He, W.-Y. & Chan, C. T. Synthetic gauge flux and Weyl points in acoustic systems. *Nat. Phys.* **11**, 920–924 (2015).



51. Rocklin, D. Z., Zhou, S., Sun, K. & Mao, X. Transformable topological mechanical metamaterials. *Nat. Commun.* **8**, 14201 (2017).
52. Yang, Z. *et al.* Topological acoustics. *Phys. Rev. Lett.* **114**, 1–4 (2015).
53. Süsstrunk, R. & Huber, S. D. Classification of topological phonons in linear mechanical metamaterials. *Proc. Natl Acad. Sci. USA* **113**, E4767–E4775 (2016).
54. Deymier, P. A., Runge, K., Swintek, N. & Muralidharan, K. Torsional topology and fermion-like behavior of elastic waves in phononic structures. *Comptes Rendus Mécanique* **343**, 700–711 (2015).
55. Bi, R. & Wang, Z. Unidirectional transport in electronic and photonic Weyl materials by dirac mass engineering. *Phys. Rev. B* **92**, 241109 (2015).
56. Berg, N., Joel, K., Koolyk, M. & Prodan, E. Topological phonon modes in filamentary structures. *Phys. Rev. E* **83**, 021913 (2011).
57. Peano, V., Brendel, C., Schmidt, M. & Marquardt, F. Topological phases of sound and light. *Phys. Rev. X* **5**, 031011 (2015).
58. Wang, Y.-T., Luan, P.-G. & Zhang, S. Coriolis force induced topological order for classical mechanical vibrations. *New J. Phys.* **17**, 073031 (2015).
59. Wang, P., Lu, L. & Bertoldi, K. Topological phononic crystals with one-way elastic edge waves. *Phys. Rev. Lett.* **115**, 104302 (2015).
60. Po, H. C., Bahri, Y. & Vishwanath, A. Phonon analog of topological nodal semimetals. *Phys. Rev. B* **93**, 205158 (2016).
61. Coulais, C., Sounas, D. & Alù, A. Static non-reciprocity in mechanical metamaterials. *Nature* **542**, 461–464 (2017).
62. Mullin, T., Deschanel, S., Bertoldi, K. & Boyce, M. C. Pattern transformation triggered by deformation. *Phys. Rev. Lett.* **99**, 084301 (2007).
63. Bertoldi, K., Reis, P. M., Willshaw, S. & Mullin, T. Negative Poisson's ratio behavior induced by an elastic instability. *Adv. Mater.* **22**, 361–366 (2010).
64. Shim, J., Perdigo, C., Chen, E., Bertoldi, K. & Reis, P. Buckling-induced encapsulation of structured elastic shells under pressure. *Proc. Natl Acad. Sci. USA* **109**, 5978–5983 (2012).
65. Florijn, B., Coulais, C. & van Hecke, M. Programmable mechanical metamaterials. *Phys. Rev. Lett.* **113**, 175503 (2014).
66. Coulais, C., Overvelde, J. T., Lubbers, L. A., Bertoldi, K. & van Hecke, M. Discontinuous buckling of wide beams and metabeams. *Phys. Rev. Lett.* **115**, 044301 (2015).
67. Fargette, A., Neukirch, S. & Antkowiak, A. Elastocapillary snapping: capillarity induces snap-through instabilities in small elastic beams. *Phys. Rev. Lett.* **112**, 137802 (2014).
68. Silverberg, J. L. *et al.* Using origami design principles to fold reprogrammable mechanical metamaterials. *Science* **345**, 647–650 (2014).
69. Kang, S. H. *et al.* Complex ordered patterns in mechanical instability induced geometrically frustrated triangular cellular structures. *Phys. Rev. Lett.* **112**, 098701 (2014).
70. Shan, S. *et al.* Multistable architected materials for trapping elastic strain energy. *Adv. Mater.* **27**, 4296 (2015).
71. Silverberg, J. L. *et al.* Origami structures with a critical transition to bistability arising from hidden degrees of freedom. *Nat. Mater.* **14**, 389–393 (2015).
72. Zhang, Y. *et al.* A mechanically driven form of kirigami as a route to 3D mesostructures in micro/nanomembranes. *Proc. Natl Acad. Sci. USA* **112**, 11757–11764 (2015).
73. Raney, J. R. *et al.* Stable propagation of mechanical signals in soft media using stored elastic energy. *Proc. Natl Acad. Sci. USA* **113**, 9722–9727 (2016).
74. Rafsanjani, A., Akbarzadeh, A. & Pasini, D. Snapping mechanical metamaterials under tension. *Adv. Mater.* **55**, 5931–5935 (2007).
75. Alexander, S. Amorphous solids: their structure, lattice dynamics and elasticity. *Phys. Rep.* **296**, 65–236 (1998).
76. van Hecke, M. Jamming of soft particles: geometry, mechanics, scaling and isotacticity. *J. Phys. Condens. Matter* **22**, 053101 (2010).
77. Katgerg, G., Tighe, B. P. & van Hecke, M. The jamming perspective on wet foams. *Soft Matter* **9**, 9759–9746 (2013).
78. Jaeger, H. M., Nagel, S. R. & Behringer, R. P. Granular solids, liquids, and gases. *Rev. Mod. Phys.* **68**, 1259 (2012).
79. Broedersz, C. P. & MacKintosh, F. C. Modeling semiflexible polymer networks. *Rev. Mod. Phys.* **86**, 995 (2014).
80. Jacobs, D. J. & Thorpe, M. F. Generic rigidity percolation: the pebble game. *Phys. Rev. Lett.* **75**, 4051–4054 (1995).
81. Wyart, M., Liang, H., Kabla, A. & Mahadevan, L. Elasticity of floppy and stiff random networks. *Phys. Rev. Lett.* **101**, 215501 (2008).
82. Ellenbroek, W. G., Zeravcic, Z., van Saarloos, W. & van Hecke, M. Non-affine response: jammed packings versus spring networks. *EPL* **87**, 34004 (2009).
83. Ellenbroek, W. G., Hagh, V. F., Kumar, A., Thorpe, M. F. & van Hecke, M. Rigidity loss in disordered systems: three scenarios. *Phys. Rev. Lett.* **114**, 135501 (2015).
84. Goodrich, C. P., Liu, A. J. & Nagel, S. R. The principle of independent bond-level response: tuning by pruning to exploit disorder for global behavior. *Phys. Rev. Lett.* **114**, 225501 (2015).
85. O'Rourke, J. *How to Fold It: The Mathematics of Linkages, Origami and Polyhedra* (Cambridge Univ. Press, 2011).
86. Grima, J. N. & Evans, K. E. Auxetic behavior from rotating squares. *J. Mater. Sci. Lett.* **19**, 1563–1565 (2000).
87. Overvelde, J. T., Shan, S. & Bertoldi, K. Compaction through buckling in 2D periodic, soft and porous structures: effect of pore shape. *Adv. Mater.* **24**, 2337–2342 (2012).
88. Overvelde, J. T. & Bertoldi, K. Relating pore shape to the non-linear response of periodic elastomeric structures. *J. Mech. Phys. Solids* **64**, 351–366 (2014).
89. Kuribayashi, K. *et al.* Self-deployable origami stent grafts as a biomedical application of Ni-rich TiNi shape memory alloy foil. *Mater. Sci. Eng. A* **419**, 131–137 (2006).
90. Song, Z. *et al.* Origami lithium-ion batteries. *Nat. Commun.* **5**, 3140 (2014).
91. Goldman, F. in *Origami<sup>2</sup>: Fifth International Meeting of Origami Science, Mathematics, and Education* (eds Wang-Iverson, P., Lang, R. J. & Yim, M.) 99–110 (CRC Press, 2011).
92. Bles, K. *et al.* Graphene kirigami. *Nature* **524**, 204–207 (2015).
93. Song, Z. *et al.* Kirigami-based stretchable lithium-ion batteries. *Sci. Rep.* **5**, 10988 (2015).
94. Xu, L. *et al.* Kirigami nanocomposites as wide-angle diffraction gratings. *ACS Nano* **10**, 6156–6162 (2016).
95. Rafsanjani, A. & Bertoldi, K. Buckling-induced kirigami. *Phys. Rev. Lett.* **118**, 084301 (2017).
96. Lamoureux, A. *et al.* Dynamic kirigami structures for integrated solar tracking. *Nat. Commun.* **6**, 8092 (2015).
97. Eidini, M. & Paulino, G. H. Unraveling metamaterial properties in zigzag-base folded sheets. *Sci. Adv.* **1**, e1500224 (2015).
98. Sussman, D. *et al.* Algorithmic lattice kirigami: a route to pluripotent materials. *Proc. Natl Acad. Sci. USA* **112**, 7449–7453 (2015).
99. Bückmann, T. *et al.* Tailored 3D mechanical metamaterials made by dip-in direct-laser-writing optical lithography. *Adv. Mater.* **24**, 2710–2714 (2012).
100. Gibson, L. & Ashby, M. *Cellular Solids: Structure and Properties* 2nd edn (Cambridge Univ. Press, 1999).
101. Wierzbicki, T. & Abramowicz, W. On the crushing mechanics of thin-walled structures. *J. Appl. Mech.* **50**, 727–734 (1983).
102. Papka, S. & Kyriakides, S. Biaxial crushing of honeycombs: — part I: experiments. *Int. J. Solids Struct.* **36**, 4367–4396 (1999).
103. Papka, S. & Kyriakides, S. In-plane biaxial crushing of honeycombs: — part II: analysis. *Int. J. Solids Struct.* **36**, 4397–4423 (1999).
104. Wu, E. & Jiang, W. Axial crush of metallic honeycombs. *Int. J. Impact Eng.* **19**, 439–456 (1997).
105. Hayes, A. M., Wang, A., Dempsey, B. M. & McDowell, D. L. Mechanics of linear cellular alloys. *Mech. Mater.* **36**, 691–713 (2004).
106. Zhang, Y. *et al.* One-step nanoscale assembly of complex structures via harnessing of an elastic instability. *Nano Lett.* **8**, 1192–1196 (2008).
107. Babaee, S., Shim, J., Weaver, J., Patel, N. & Bertoldi, K. 3D soft metamaterials with negative Poisson's ratio. *Adv. Mater.* **25**, 5044–5049 (2013).
108. Bertoldi, K. & Boyce, M. C. Mechanically-triggered transformations of phononic band gaps in periodic elastomeric structures. *Phys. Rev. B* **77**, 052105 (2008).
109. Wang, P., Casadei, F., Shan, S., Weaver, J. & Bertoldi, K. Harnessing buckling to design tunable locally resonant acoustic metamaterials. *Phys. Rev. Lett.* **113**, 014301 (2014).
110. Shan, S. *et al.* Harnessing multiple folding mechanisms in soft periodic structures for tunable control of elastic waves. *Adv. Funct. Mater.* **24**, 4935–4942 (2014).
111. Krishnan, D. & Johnson, H. Optical properties of two dimensional polymer photonic crystals after deformation induced pattern transformations. *J. Mech. Phys. Solids* **57**, 1500–1513 (2009).
112. Li, J. *et al.* Switching periodic membranes via pattern transformation and shape memory effect. *Soft Matter* **8**, 10322–10328 (2012).
113. Kang, S. *et al.* Buckling-induced reversible symmetry breaking and amplification of chirality using supported cellular structures. *Adv. Mater.* **25**, 3380–3385 (2013).
114. Bazant, Z. P. & Cedolin, L. *Stability of Structures: Elastic, Inelastic, Fracture, and Damage Theories* (Oxford Univ. Press, 1991).
115. Pandey, A., Moulton, D., Vella, D. & Holmes, D. Dynamics of snapping beams and jumping poppers. *EPL* **105**, 24001 (2014).
116. Restrepo, D., Mankame, N. D. & Zavattieri, P. D. Phase transforming cellular materials. *EML* **4**, 52–60 (2015).
117. Hasan, M. Z. & Kane, C. L. Colloquium: topological insulators. *Rev. Mod. Phys.* **82**, 3045–3067 (2010).
118. Lubensky, T. C., Kane, C. L., Mao, X., Souslov, A. & Sun, K. Phonons and elasticity in critically coordinated lattices. *Rep. Prog. Phys.* **78**, 073901 (2015).
119. Zhou, Y., Chen, B. G., Upadhyaya, N. & Vitelli, V. Kink-antikink asymmetry and impurity interactions in topological mechanical chains. *Phys. Rev. E* **95**, 022202 (2017).
120. Mitchell, N. P., Nash, L. M., Hexner, D., Turner, A. & Irvine, W. T. M. Amorphous gyrosopic topological metamaterials. Preprint at <https://arxiv.org/abs/1612.09267> (2016).
121. Souslov, A., van Zuiden, B. C., Bartolo, D. & Vitelli, V. Topological sound in active-liquid metamaterials. *Nat. Phys.* <http://dx.doi.org/10.1038/nphys4193> (2017).
122. Coulais, C., Kettenis, C. & van Hecke, M. A characteristic length scale causes anomalous size effects and boundary programmability in mechanical metamaterials. *Nat. Phys.* <http://dx.doi.org/10.1038/nphys4269> (2017).
123. Lang, R. J. in *Proc. 12th Ann. Symp. Comp. Geo.* (eds Whitesides, S. H.) 98–105 (ACM, 1996).
124. Felton, S., Tolley, M., Demeine, A., Rus, D. & Wood, R. A method for building self-folding machines. *Science* **345**, 644–646 (2014).
125. Zeravcic, Z., Manoharan, V. N. & Brenner, M. P. Size limits of self-assembled colloidal structures made using specific interactions. *Proc. Natl Acad. Sci. USA* **111**, 15918–15923 (2014).
126. Miskin, M. Z. & Jaeger, H. M. Adapting granular materials through artificial evolution. *Nat. Mater.* **12**, 326–331 (2013).

#### Acknowledgements

J.C. acknowledges support from the European Research Council (ERC) through the Starting Grant No. 714577 PHONOMETA and from the Ministerio de Economía, Industria y Competitividad (MINECO) through a Ramon y Cajal grant (Grant No. RYC-2015-17156). M.vH. acknowledges funding from the Netherlands Organisation for Scientific Research through Grant VICI No. NWO-680-47-609. V.V. acknowledges support from the University of Chicago Materials Research Science and Engineering Center, which is funded by the National Science Foundation through Grant No. DMR-1420709.

#### Author contributions

All authors contributed equally to the preparation of this manuscript.

#### Competing interests statement

The authors declare no competing interests.

#### Publisher's note

Springer Nature remains neutral with regard to jurisdictional claims in published maps and institutional affiliations.

#### How to cite this article

Bertoldi, K. *et al.* Flexible mechanical metamaterials. *Nat. Rev. Mater.* **2**, 17066 (2017).

#### FURTHER INFORMATION

Shape-transforming art: <https://vimeo.com/36122966>